Chapter 3

Nematic – Nematic transition in highly polar compounds

3.1 Introduction

In the previous chapter we have shown that under compression the orientational order parameter S of the mesophase increases with increasing pressure. In this chapter we discuss the effect of pressure on N-N transition in a pure nematogen. We also present the evidence for an N-N transition at atmospheric pressure in a binary mixture of polar compounds.

Highly polar compounds exhibit very interesting phase sequences like smectic polymorphism, the reentrant nematic phase and double reentrance, etc [1,2]. Both phenomenological and molecular theoretical models have been developed to explain these phenomena [1]. In uniaxial nematics (N) the long axes of the molecules are oriented on the average about the director $\hat{n}$, which is a dimensionless apolar unit vector. The apolar nature of the director in nematogens with highly polar end groups can be understood as the molecules have an anti-parallel short-range order in the medium [3]. Smectic A (SmA) liquid crystals have a layering order, with the layer normal ($\hat{z}$) being parallel to $\hat{n}$. In polar compounds which exhibit reentrant N and SmA phases, the high temperature smectic A_d (SmA_d) phase has a partial bilayer order with $l < d < 2l$, where l is the molecular length and d the layer spacing. The low temperature Smectic A_1 (SmA_1) phase has a layer spacing equal to the monomolecular length i.e., $d = l$. The unusual phenomena exhibited by highly polar compounds have been successfully explained by Prost and co-workers using a phenomenological Landau theory. This model [1] takes into account the coupling between the two smectic order parameters corresponding to the two lengths mentioned above. One of the consequences of this model is the prediction of an N_d to N_1 transition line in continuation of the SmA_d to SmA_1 transition line, the latter being characterised by an appropriate jump in the layer spacing. Analogous to the divergence of compressibility of a liquid at the liquid-gas critical point the inverse of the layer compressional elastic modulus B is predicted to vanish at the SmA_1-SmA_d (or SmA_d-SmA_2) critical point [4]. Prost et al [5] have measured the value of B in a binary mixture of polar compounds exhibiting SmA_d-SmA_2 transition. They report that B vanishes at SmA_d-SmA_2 critical point as theoretically predicted. In analogy

with this the curvature elastic constant of the nematic medium may be expected to vanish at the N_1N_d critical point. Indeed such an N-N transition has been found as a continuation of the SmA_1-SmA_d transition line in the concentration-temperature phase diagram of a binary mixture of polar compounds [6]. Nounesis et al have conducted AC calorimetric measurements and high resolution X-ray scattering studies on a binary mixture of polar compounds with various concentrations which exhibit SmA_d-N-SmA_1 transition [6]. They report that in binary mixtures of two different concentrations within a narrow range, the specific heat C_p exhibits three distinct peaks characterising the phase sequence SmA_d-N_d-N_1-SmA_1 (see Figure 3.1). The strong peak corresponding to N_1N_d transition indicates that the N_1N_d transition is associated with strong fluctuations.

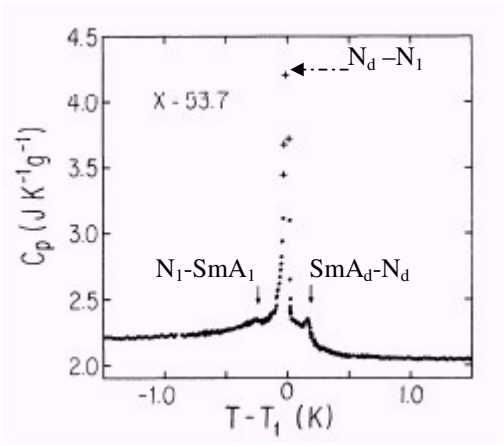

Figure 3.1: The variation of specific heat C_p in a narrow temperature region for a binary mixture of polar compounds exhibiting the phase sequence: SmA_d-N_d-N_1-SmA_1. The temperature indicated as T_1 corresponds to the temperature at which a peak is observed signifying the N_1N_d transition (indicated by horizontal arrow). The vertical arrows indicate SmA_d-N_d and N_1-SmA_1 transitions. (adapted from reference [6]).

The high resolution X-ray scattering studies on this system have revealed that the N_d-N_1 transition is a weak first order transition characterised by a discontinuous jump in the correlation lengths associated with short-range smectic fluctuations. However, optical microscopic observations did not reveal any visible change at the N_d-N_1 transition. This transition is a weak first order transition as the macroscopic symmetry of the two nematics is identical. As in the liquid-gas transition under varying

pressures the N_d-N_1 transition line can end in a critical point beyond which the two phases can evolve into each other as physical parameters such as concentration in a mixture or pressure and temperature are varied.

Prost and Toner using a fluctuation corrected mean field theory [7] based on dislocation loop melting of SmA have stated that over 150 topologically distinct phase diagrams with fluctuation induced nematic regions that are consistent with their theory are possible. Two such possible topologies are shown in Figure 3.2. The diagrams indicate the possibility of *two* N-N transitions in an appropriate parameter space.

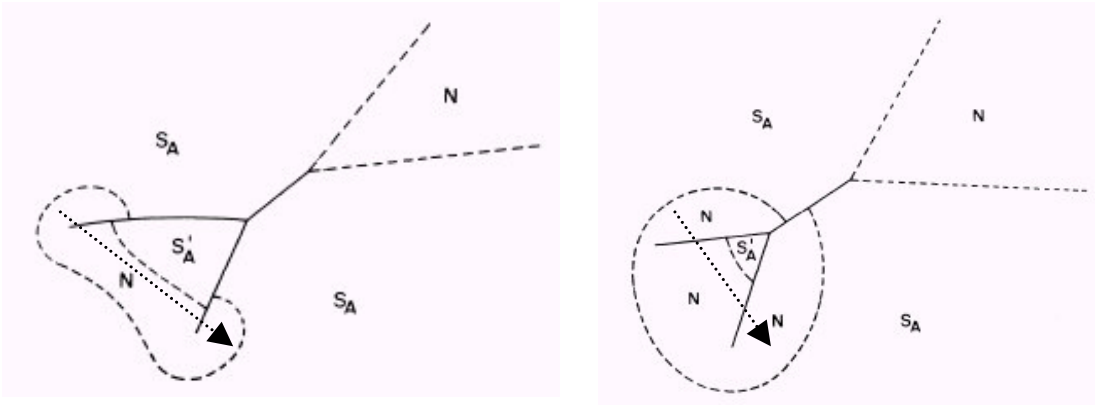

Figure 3.2: Two topologies out of the 150 possible topologies predicted by Prost and Toner (adapted from reference [7]). The solid and dashed lines represent first and second order phase transitions. The dotted lines with arrows indicate the possibility of <u>two</u> N-N transitions.

The physical origin of the two lengths corresponding to SmA_d and SmA_1 phases has been explained in a molecular model proposed by Madhusudana et al [8]. In highly polar compounds the electrostatic interaction between the polar groups of neighbouring molecules favours an antiparallel association [3]. The aromatic cores of the molecules have large polarizabilities and the strong dispersion interaction between such cores of neighbouring molecules leads to an antiparallel association as shown in Figure 3.3a. In this configuration the effective dipole moment of the molecule is enhanced, as the neighbouring molecule induces a dipole moment which is parallel to the dipole moment of the polar group of the given molecule. The aliphatic chains are

so far apart that the dispersion interaction between the chains of neighbours is negligible. When the neighbouring molecules are parallel to each other as in Figure 3.3b the dipolar interaction is repulsive, but the net dipole moment of a molecule is reduced as the induced dipole due to the neighbouring molecule is in a direction opposite to that of the permanent dipole of the given molecule. In addition, the chains are in close proximity, adding to the attractive interaction. The dipole-induced dipole interaction as well as the interchain dispersion interaction vary as $1/r^6$, where r is the intermolecular distance. On the other hand the permanent dipole-dipole interaction varies as $1/r^3$.

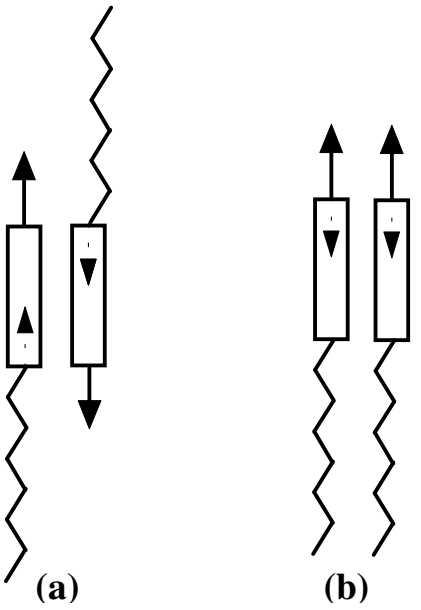

Figure 3.3: Schematic representation of intermolecular associations of neighbouring molecules with highly polar cyano end groups: (a) antiparallel configuration favoured at low densities (b) parallel configuration favoured at high densities (the permanent and induced dipoles are indicated respectively by solid and dashed lines with arrows).

At low densities the permanent dipole-dipole interaction is dominant leading to the antiparallel arrangement of neighbouring molecules. As the density is increased either by reducing temperature or by increasing pressure, r decreases and a change in the intermolecular configuration from antiparallel to parallel association of molecules can take place. This leads to a *polar short range* order in the medium. Indeed such a polar short-range order has been detected by Basappa *et al* in a strongly polar nematogen, viz., p-cyanophenyl p-n-heptyl benzoate (CP7B) [9]. This compound has the following phase sequence: crystal - 43.5 ^{0}C - N - 56 ^{0}C - Isotropic (I), and the nematic

phase can be supercooled to room temperature. Basappa et al [9] also noticed a sharp increase in the intensity of light scattered by twist fluctuations in the medium around 33 ^{0}C when a 10 µm thick sample was cooled under a high electric field of ~ 600 esu (Figure 3.4).

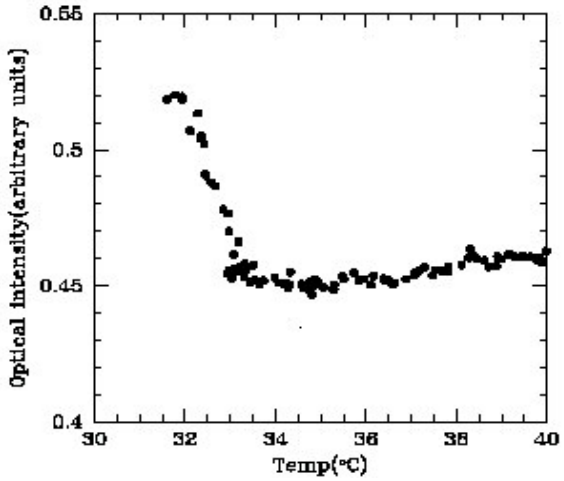

Figure 3.4: Temperature variation of the light scattered from twist fluctuations in a 10 µm thick sample of CP7B subjected to 180 V, frequency = 4.11 kHz (adapted from reference 9).

They report that the conoscopic observations on samples of thickness ~ 40µm under a similar field indicates that the medium continues to be uniaxial below this temperature. When planar aligned samples were subjected to a transverse field of a similar magnitude in a gap etched in an ITO coated plate, they did not find any evidence of a transition to the SmA phase by direct texture observations [9]. They speculated that this indicated a nematic-nematic (N-N) transition in the compound.

Indeed an extension of the molecular theory of liquid crystal phases exhibited by highly polar compounds proposed by Govind et al [10] has predicted the possibility of such an N-N transition which is not associated with the SmA phase. The model shows that the N_1-N_d transition temperature increases with pressure [11] and the first order N_1-N_d transition line ends in a critical point. Experiments by Sobha et al [12] on *planar aligned thin* samples of CP7B, with thickness lying between 1.9 µm and 3 µm revealed a jump in the optical path difference at some temperature in the

nematic range (Figure 3.5). They identified the relevant event as an N-N transition. The transition temperature decreased with increase in sample thickness.

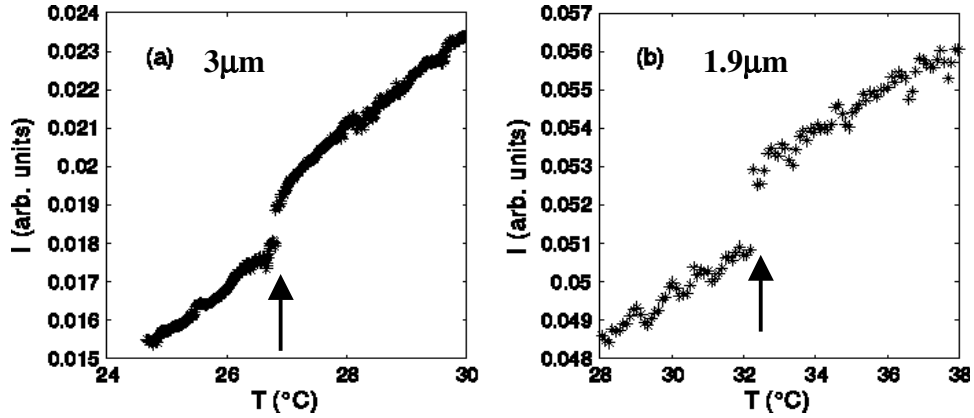

Figure 3.5: Transmitted intensity profiles as a function of temperature for cells of thicknesses of (a) 3 μm and (b) 1.9 μm respectively (reference 12). Arrows indicate the jump in the transmitted intensity at the N-N transition. Note that T_{NN} is larger for 1.9 μm cell compared to that of 3 μm cell.

In both thin cells, as well as samples subjected to high electric fields, [9,12] the orientational order parameter is enhanced, compared to that in a field-free thick sample. It is hence likely that in CP7B the N-N transition occurs in the bulk at a temperature well below the ambient when the order parameter increases to the required value.

The transition point can be expected to increase above the ambient temperature at elevated pressures. To check this possibility, we undertook high pressure (HP) studies on this compound. The N-N transition is a very weak first order transition with about 1% jump in the orientational order parameter, when the latter has a sufficiently large value [12]. We have conducted the optical path-difference measurements on planar aligned samples of CP7B as functions of both temperature and pressure. Using the intensity data the birefringence, $\Delta\mu$ has been evaluated as functions of both temperature and pressure using the method explained in Chapter 2 (see section 2.29). We have found that indeed the N-N transition occurs in the bulk CP7B sample of thickness ~12 μm at high pressures.

It is convenient to have a system which exhibits the N-N transition at atmospheric pressure at temperatures well above the ambient so that many other experiments can be conducted. We have found that certain binary mixtures of polar compounds exhibit such behaviour. We have prepared binary mixtures of CP7B with another polar compound 4-[5-(4-Butyl-phenyl)-pyrimidin-2-yl]-benzonitrile (4PCPP). In a binary mixture of 70.5 mol% of CP7B with 4PCPP we observed the signature of N-N transition above the ambient temperature. We have also found that the N-N transition temperature is strongly dependent on the thickness of the sample.

3.2 Experimental

The chemical structures and the transition temperatures of the compounds used in the study are as shown in Figure 3.6. All the three compounds were got from Messrs F. Hoffman La Roche & Co. Limited .

(a) CP7B

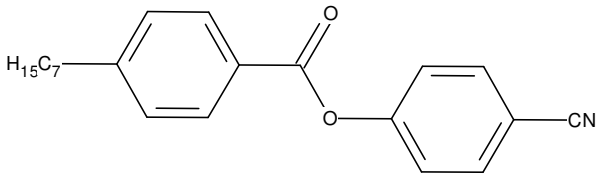

Cr - 44 ^{0}C - N - 56.5 ^{0}C - I

(b) CP6B

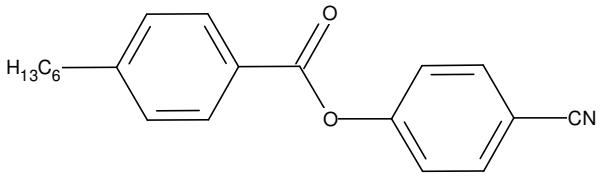

Cr - 44.5 ^{0}C - N - 47.5 ^{0}C - I

(c) 4PCPP

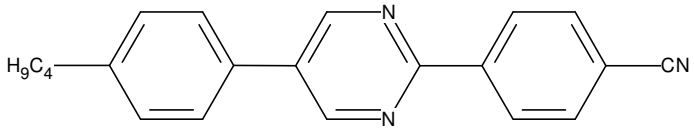

Cr - 93.5 ^{0}C - N - 244.7 ^{0}C - I

Figure 3.6: Chemical Structures and transition temperatures of CP7B, CP6B and 4PCPP.

The optical phase difference measurements on CP7B at elevated pressures were carried out using the experimental technique explained in chapter 2 (section 2.2). The experimental measurements on some binary mixtures of polar compounds exhibiting N-N transition at atmospheric pressure were conducted using an experimental procedure described below.

The cells were prepared using ITO coated glass plates which are etched as shown in Figure 1.13. (Chapter 1). The etched glass plates were coated with polyimide and cured for about an hour at 280 ^{0}C. The polyimide coated plates were rubbed unidirectionally with soft tissue paper to get a homogeneous alignment of nematic director. By spreading an epoxy glue mixed with glass beads on either side of the region outside the electrode area, cells of required thickness were prepared and cured for about an hour at 150 ^{0}C. In case of cells of thickness $t > 12$ μm, mylar spacers were used to fix the thickness of the cell. The thickness of the cell was measured at many positions within the electrode area using the Ocean Optics spectrometer. Many cells were prepared at a time and cells with uniform thickness were chosen for the experiment. For cells of thickness $t < 12$ μm the thickness was found to be constant to within 0.5%. But for cells of $t > 12$ μm, prepared using mylar spacers, the cell thickness was constant to within ~ 4%. The sample is filled into the cell in the isotropic phase. An electric field can be applied between the ITO plates and the Freedericks transition experiments can also be carried out on the planar sample.

A schematic representation of the experimental setup is shown in Figure 3.7. The sample is mounted in a hot stage (Instec HS1) placed on the rotating stage of a polarising microscope (Leitz, Orthoplan). The temperature of the sample mounted in the hot stage is controlled by Instec MK1 temperature controller to an accuracy of 10 mK. A platinum resistance thermometer placed close to the sample is used to measure the temperature of the sample. A He- Ne laser beam with wavelength of 633nm (Oriel; 3mW) is allowed to pass through a beam splitter and split into two beams. One of the beams is made to pass through the sample kept between crossed polarisers and the transmitted intensity is detected using a photodiode (PD1: Centronics model OSD-5). The stability of laser beam is monitored using a reference photodiode (PD2). Outputs of both the photodiodes are monitored using a multimeter (MUL: Keithley

model 2000). For conducting Freedericks transition experiments on the nematic sample an appropriate electric field was applied using a lock-in amplifier (LIA: model SRS830 DSP lock-in amplifier).

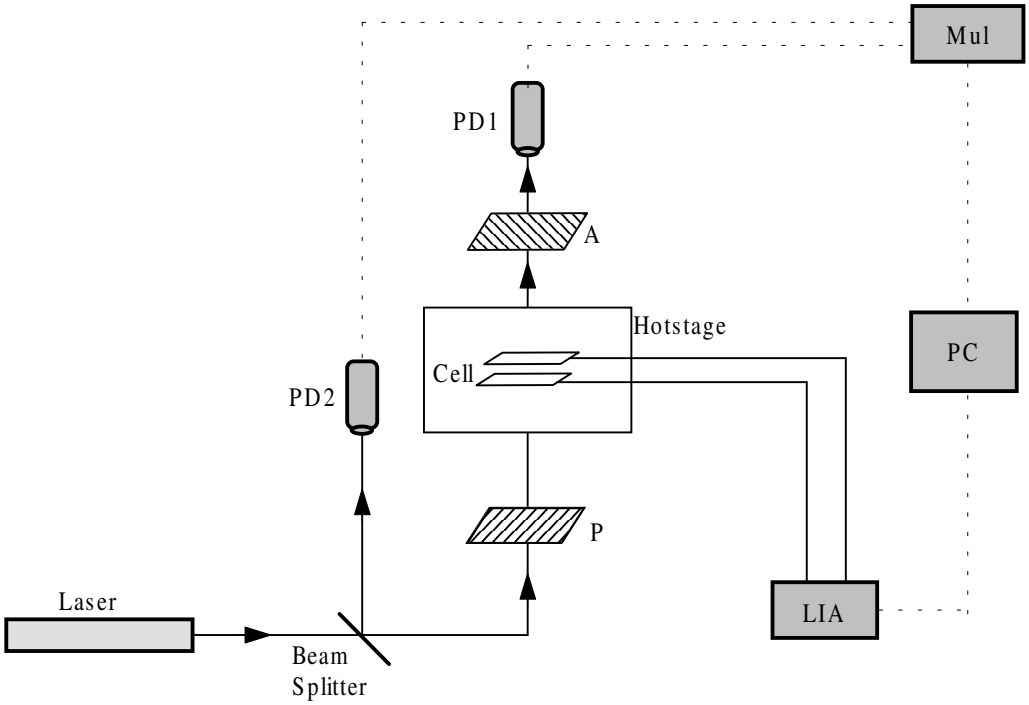

Figure 3.7: Schematic representation of experimental setup: Mul-Multimeter (Keithley model 2000), PD1 and PD2 – photodiodes, P-Polariser, A- Analyser, LIA-lock-in amplifier.

The rotating stage of the microscope is used to locate the orientation at which the sample appears dark between crossed polarisers. This orientation corresponds to the one at which the rubbing direction is parallel to one of the crossed polarisers. The rotating stage of microscope is then rotated such that the rubbing direction of the sample is at an angle of 45^0 with crossed polarisers. The transmitted intensity in this setting corresponds to maximum sensitivity and is given by $I=I_0(1-cos\Delta\phi)/2$, where $\Delta\phi=2\pi\Delta\mu t/\lambda$ is the optical phase difference and I_0 the intensity of the polarised beam incident on the sample. $\Delta\mu=\mu_e-\mu_o$, where μ_e and μ_o are the principal refractive indices of the nematic, t the sample thickness and λ the wavelength of incident light. A suitable software program is used to record the intensity as a function of

temperature. The transmitted intensity is recorded at temperature intervals of 0.2 ^{0}C. In thick cells the transmitted intensity profile as a function of temperature shows a number of maxima and minima. The order of the maximum is determined using Freedericks transition technique (see section 1.25, chapter 1). Using the value of measured thickness *t* of the cell the birefringence $\Delta\mu$ can be estimated.

3.3 Results and Discussion

3.31 HP measurements on CP7B

The profile of the ratio of transmitted to reference intensity signals at 650bars is shown in Figure 3.8. The value of the measured transmitted intensity is zero in the isotropic phase as expected. However, the minima in the nematic phase have finite values of intensity indicating that the thickness has a gradient in the sample area ~5 mm^2 illuminated by the laser beam. The estimated average thickness *t* of the sample is ~12.6 μm and the estimated gradient in thickness of the sample as discussed in chapter 2 is ~11%. The N-N transition temperature is strongly dependent on the thickness of the sample [12], as will be discussed in next chapter. As such, the transition is not sharp and it appears as a small jump in the intensity profile at 39.6 ^{0}C.

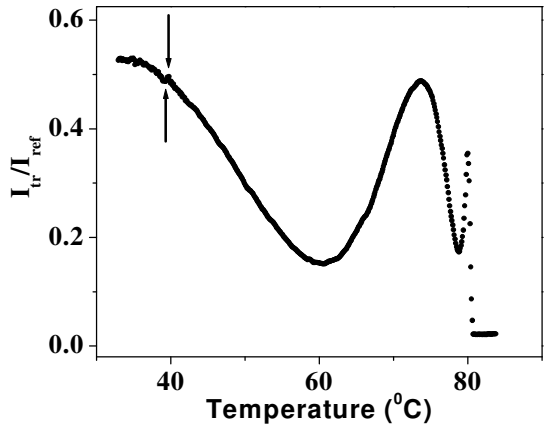

Figure 3.8: The variation of the ratio of transmitted intensity to reference intensity with temperature in CP7B at the pressure of 650 bars. The N-N transition is indicated by arrows.

At higher pressures, T_{NN} increases and the temperature gradient across the sample also increases. As a consequence the N-N transition gets smeared out, and the

transition is seen as a slope change in the intensity. The data at 1.3 kbar is shown in Figure 3.9 where the slope change around 49.2 ^{0}C is indicated by arrows.

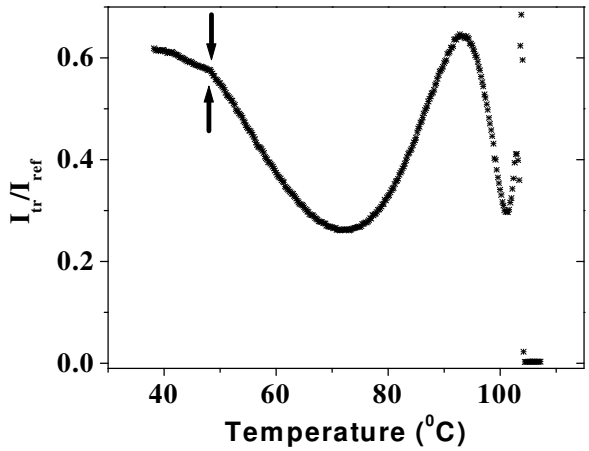

Figure 3.9: The variation of the ratio of transmitted intensity to reference intensity with temperature at the pressure of 1.3 kbar. The N-N transition is indicated by arrows.

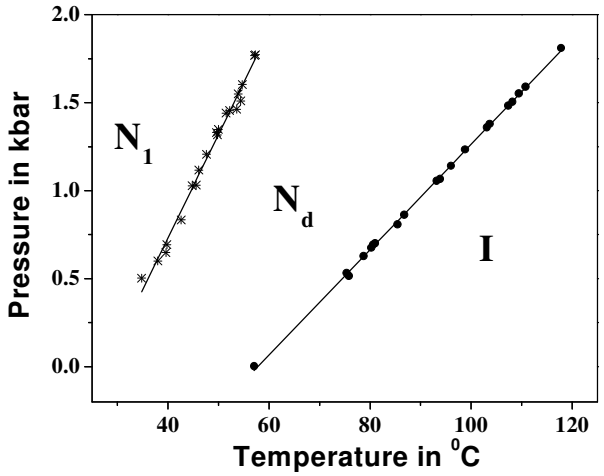

Figure 3.10: The pressure-temperature phase diagram of CP7B. The nematic phase occurring at temperatures above T_{NN} is indicated by N_d and that at lower temperatures by N_1.

The pressure – temperature phase diagram of CP7B is shown in Figure 3.10 in which both the N-N and NI transition temperatures are plotted as functions of pressure. The nematic phase occurring above T_{NN} is denoted as N_d, and that occurring below T_{NN} as N_1 where the subscripts d and 1 indicate the type of short range order favoured. Both T_{NI} and T_{NN} vary linearly with pressure with the corresponding slopes dP/dT being 30 bar/^{0}C and 58.9 bar/^{0}C respectively. We do not show the melting transition temperature as a function of pressure, as the sample always supercooled at any given pressure. The values of the jump in the volume ($\Delta V/V=0.3\%$) [13] and the heat of NI transition ΔH (=1 KJ/mole) [14] of CP7B at atmospheric pressure are available in the literature. Using the Claussius-Clapeyron equation viz., $(dP/dT) = \Delta H/(\Delta V T_{NI})$, we obtain $dP/dT_{NI} = 33$ bar/^{0}C which agrees well with the experimental value. Of course such data are not available for the N-N transition. We have estimated the optical phase difference, $\Delta\phi = 2\pi\Delta\mu t/\lambda$ of the sample using the measured optical intensity profiles at various pressures. Using the refractive indices data at atmospheric pressure available in the literature [15], the sample thickness t and the absolute values of the phase difference corresponding to the maxima and minima of the measured optical intensity have been estimated. The temperature variation of $\Delta\mu$ calculated from the intensity data at atmospheric pressure is in agreement (to <1.5%) with that obtained by Zeminder et. al [15] as shown in Figure 3.11.

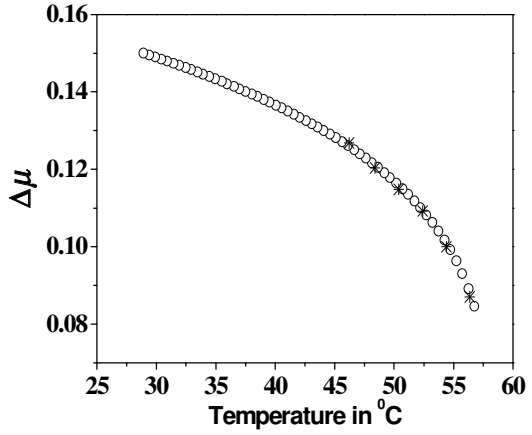

Figure 3.11: Temperature variation of birefringence $\Delta\mu$ of CP7B at ambient pressure. The open circle corresponds to our measurement and ✳ are taken from reference [15] of refractive indices measurement.

The birefringence $\Delta\mu$ at various pressures are evaluated using the intensity data assuming that the sample thickness *t* remains constant at all applied pressures. The variations of $\Delta\mu$ as functions of temperature along various isobars are presented in Figure 3.12. The orientational order parameter *S* of nematic increases with increasing pressure as the intermolecular distance *r* decreases at any temperature. Hence, $\Delta\mu$ which is a measure of *S* is correspondingly enhanced with increasing pressure, as can be seen in Figure 3.12. The $\Delta\mu$ value corresponding to T_{NN} at elevated pressures is 0.165 (±2%), which is in agreement with the $\Delta\mu$ value measured by Sobha et al [12] in a cell of thickness 1.5 μm at the temperature corresponding to T_{NN}.

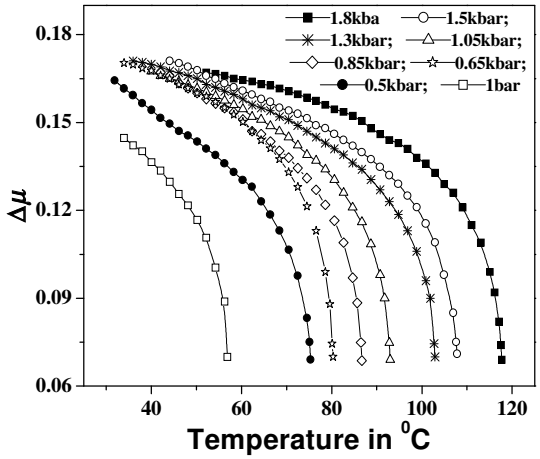

Figure 3.12: Temperature variations of the birefringence $\Delta\mu$ of CP7B at various pressures.

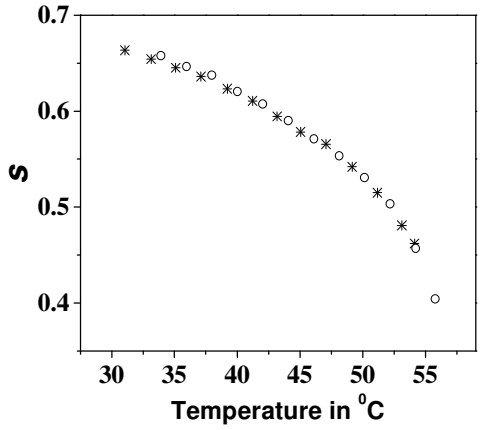

Figure 3.13: Temperature variation of orientational order parameter *S* of CP7B at atmospheric pressure. The symbols ○ and ✳ correspond to our measurement and NMR measurements by Balakrishnan et al [17] respectively.

We have fitted the $\Delta\mu$ values at atmospheric pressure to Haller's extrapolation formula (see quation 2.6) [16] and estimated the value of $\Delta\mu_0$ (= 0.22) and used it to calculate S values. The temperature variation of S at atmospheric pressure agrees (to <1.5%) with the measurement of Balakrishnan et al [17] using the NMR technique as shown in Figure 3.13. We have also fitted the $\Delta\mu$ values along each isobar to Haller's extrapolation formula (see equation 2.6). For all applied pressures the estimated value of $\Delta\mu_0 \approx 0.22$. The estimated values of T^*, the exponent β and $\Delta\mu_0$ are tabulated along with T_{NI} in Table1. The value of T^*-T_{NI} decreases from 1.6 ^{0}C at atmospheric pressure to $\approx$ 0.5 ^{0}C at elevated pressures, and the exponent β varies from 0.20 to 0.17.

Pressure in bars	T_{NI} (K)	T^*(K)	β	$\Delta\mu_0$
1	329.9	331.5	0.20	0.22
500	348.4	349.1	0.20	0.22
650	353.3	353.8	0.17	0.22
850	359.6	360.1	0.17	0.21
1050	365.9	366.3	0.17	0.21
1300	375.9	376.4	0.18	0.21
1500	380.9	381.4	0.18	0.21
1800	390.7	391.1	0.18	0.22

Table 1: Estimated values of T^*, the exponent β and $\Delta\mu_0$ for CP7B at various pressures estimated using Haller's extrapolation formula.

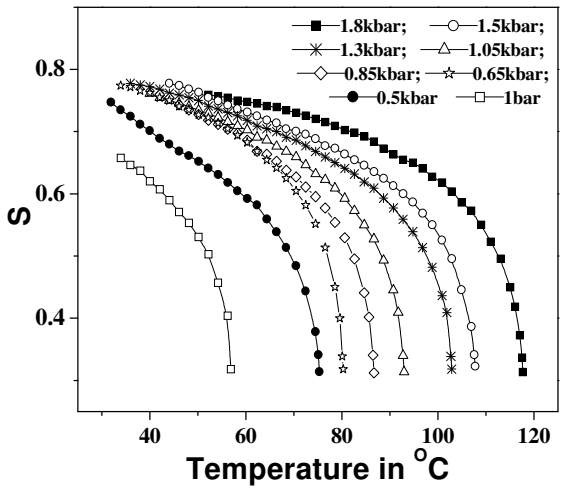

Figure 3.14: Temperature variations of the orientational order parameter S of CP7B at various pressures.

The temperature variations of S along various isobars are presented in Figure 3.14, in which it can be seen that the value at the NI transition point, i.e., $S_{NI,}$ is practically *constant*, and equal to 0.32 (±1.5%) at all the applied pressures. This is in agreement with the earlier results on Paraazoxyanisole (PAA) using NMR measurements at high pressures [18]. Wallis et al [19] have also found that the values of S_{NI} remain constant for several (but not all) nematogens at different pressures. Indeed the mean field theories such as the Maier-Saupe theory and the one outlined by Deloche et al of NI transition [1,18] predict that the value of S_{NI} should be independent of pressure along the transition line. It is indeed interesting to note that the value of S at the N-N transition (S_{NN}) is also a constant and is = 0.75 ±0.01 in the range of pressures from 0.6 to 1.8 kbar. The theoretical studies on this transition do not address this question. As seen in Figures 3.12 and 3.14, a much larger increase in temperature is needed to compensate for an increase in pressure to maintain a low value of the order parameter which occurs at a low density, than that for a high value of S. This is indeed reflected in the very different slopes measured for dP/dT_{NN} and dP/dT_{NI} as seen in Figure 3.10. Indeed the molecular theory of liquid crystal phases exhibited by highly polar compounds proposed by Govind et al [11] shows that the N-N transition temperature increases linearly with increasing pressures. However as the theoretical model takes into account hard rod interactions restricted only up to the second virial term, the estimated dP/dT_{NN} is much smaller than the experimentally observed value.

Our results confirm the suggestion from earlier experimental investigations that the N-N transition occurs in CP7B, at a sufficiently large value of the order parameter [12]. Our experiments also show that both the N-I and N-N transitions occur at fixed values of the order parameters, which are independent of pressure.

3.32 N-N transition in binary mixtures of polar compounds at atmospheric pressure

It is interesting to have systems exhibiting N-N transition at atmospheric pressure in a convenient temperature range. With this aim, we have prepared some binary mixtures of polar compounds. The nematogen CP7B (See Figure 3.6a) has a highly polar cyano end group and the ester linkage between the phenyl rings adds to the dipole moment of the molecule enhancing its magnitude. As already discussed CP7B exhibits N-N transition at temperatures above ambient at atmospheric pressure in planar aligned *thin* cells. In the bulk CP7B exhibits N-N transition only either on application of high electric field or at elevated pressures. The pure nematogen 4PCPP (see Figure 3.6c) also has a cyano end group and the pyramidine ring which connects the two phenyl rings enhances the dipole moment leading to a large longitudinal dipole moment of the molecule. Further, it has a wide nematic range (See Figure 3.6). We have conducted the optical path difference measurements on two binary mixtures of CP7B with 4PCPP.

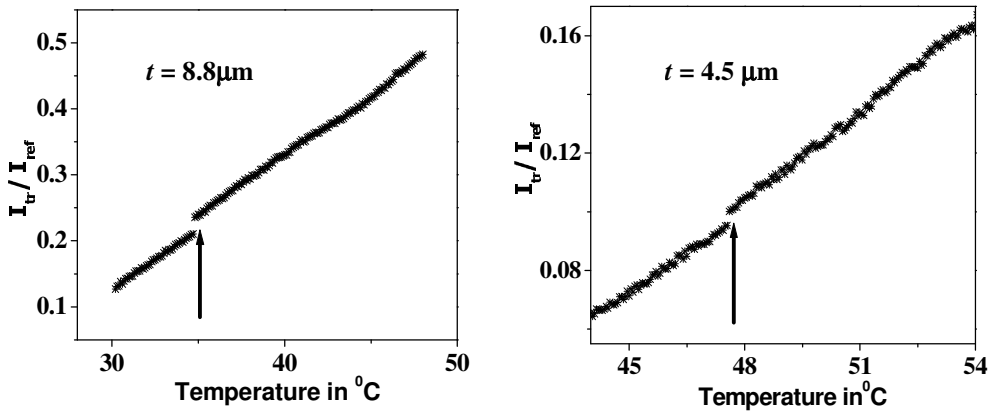

Figure 3.15: Temperature variations of transmitted intensity to reference intensity for 70.5 mol % of CP7B with 4PCPP in cells of thickness 8.8 μm and 4.5 μm respectively. Note the jump in intensity at 34.8 ^{0}C and 47.5 ^{0}C in cells of t = 8.8 μm and t = 4.5 μm respectively indicated by arrows.

The mixture with 73 mol% of CP7B exhibits the NI transition at 102 ^{0}C. Optical path difference measurements on this mixture in a 8μm cell did not reveal any N-N transition. The mixture with 70.5 mol% of CP7B with 4PCPP has T_{NI} = 106.3 ^{0}C, and exhibits the N-N transition. The temperature variations of transmitted intensity of *planar* aligned cells of thicknesses 8.8μm and 4.5μm are shown in Figure 3.15 for this mixture in a temperature range close to the N-N transition.

It can be seen that there is a jump in the intensity signifying N-N transition at 34.8 ^{0}C and 47.5 ^{0}C in cells of thicknesses 8.8 μm and 4.5 μm respectively. It may be noted that the N-N transition temperature increases with decreasing thickness of the sample in agreement with the earlier studies on a pure compound [12]. As the compound CP7B was in short supply, we did not carry out further studies on this binary mixture.

CP6B (see Figure 3.6b), the lower homologue of CP7B also has a large longitudinal dipole moment, but a very narrow nematic range. We have conducted extensive experimental studies on binary mixtures with various concentrations of 4PCPP with CP6B. The results are discussed in the next chapter. X-ray studies and the dielectric measurements on this system however indicate that the N-N transition observed in this mixture is a new type of N-N transition and does not correspond to the N_1N_d transition. As such, even the N-N transition seen in the binary mixtures of CP7B with 4PCPP seen in Figure 3.15 may not correspond to the N_1N_d transition seen in pure CP7B.

3.4 Conclusions

We have observed an N-N transition in the *bulk* (t ~12 μm) of pure CP7B at *elevated* pressures. We show that the order parameter S at both NI and N-N transition remain constant independent of pressure. We have also observed an N-N transition in *binary mixtures* of highly polar compounds at *atmospheric pressure* at temperatures above ambient.

References

1. P. G. de Gennes and J. Prost, *The Physics of Liquid Crystals*, Clarendon Press, Oxford, 1993.

2. S. Chandrasekhar, *Liquid Crystals*, Cambridge University Press, Cambridge, 1992.

3. N.V. Madhusudana and S. Chandrasekhar, "The role of permanent dipoles in nematic order", *Pramana* (*Suppl.*) **1**, 57-68, 1975.

4. Y. Park, T.C. Lubensky, P. Barois and J. Prost, "New critical point in smectic liquid crystals", *Phys. Rev. A* **37**, 2197-2213, 1988.

5. J. Prost, J. Pommier, J.C. Rouillon, J.P. Marcerou, P.Barois, M. Benzekri, A. Babeau and H.T. Nguyen, "Critical behavior of the layer-compressional elastic modulus at a smectic-smectic isolated critical point", *Phys. Rev. B* **42**, 2521-2525, 1990.

6. G. Nounesis, C.W. Garland and R. Shashidhar, "Crossover from three-dimensional XY to tricritical behavior for the nematic-smectic-A1 phase transition", *Phys. Rev. A*, **43**, 1849-1856, 1991; G. Nounesis, S. Kumar, S. Pfeiffer, R. Shashidhar and C.W. Garland, "Experimental Observation of a Transition between Two Uniaxial Nematic Liquid-Crystal Phases", *Phys. Rev. Lett.,* **73**, 565-568, 1994.

7. J. Prost and J. Toner, "Dislocation-loop melting theory of phase diagrams with nematic regions surrounded by smectic regions", *Phys. Rev. A* **36**, 5008-5014, 1987.

8. N.V. Madhusudana and Jyotsna Rajan, "A simple molecular theory of double reentrance exhibited by highly polar compounds", *Liq. Cryst.* **7**, 31- 40, 1990.

9. G. Basappa and N.V. Madhusudana, "Effect of a strong electric field on a nematogen: evidence for polar short range order", *Eur. Phys. J. B* **1**, 179-187, 1998.

10. A.S. Govind and N. V. Madhusudana, "A simple molecular theory of a nematic-nematic phase transition in highly polar compounds", *Liq. Cryst.* **14**, 1539-1551, 1993; A.S. Govind, "Theoretical Studies on Phase Transitions in Liquid Crystals", *Ph.D. Thesis*, Bangalore University, 2003.

11. A.S. Govind and N.V. Madhusudana, "A molecular theory including hard rod interactions of liquid crystalline phases exhibited by highly polar compounds", *Liq. Cryst.* **27**, 1249-1258, 2000.

12. Sobha R Warrier, D. Vijayaraghavan and N.V. Madhusudana, "Evidence for a nematic-nematic transition in thin cells of a highly polar compound", *Europhys. Lett.* **44**, 296-301, 1998.

13. A.G. Shashkov, I.P. Zhuk and V.A. Karolik, "Calculation of some thermodynamic properties of liquid-crystal compounds", *High Temp. High Pressures* **11**, 485-490, 1979.

14. George W. Smith, "Thermal parameters of some Liquid crystals", *Mol. Cryst. Liq. Cryst*. **41,** 89-95, 1977.

15. A.K. Zeminder, S. Paul and R. Paul, "Refractive Indices and Orientational Order Parameter of Five Liquid Crystals in Nematic Phase", *Mol. Cryst. Liq. Cryst*. **61**, 191-206, 1980.

16. I. Haller, "Thermodynamic and static properties of liquid crystals", *Prog. Solid State. Chem*. **10**, 103-118, 1975.

17. N.S. Balakrishnan, J.P Bayle, Mei-sing Ho, Son C. Pham and B.M. Fung, "Determination of the orientational ordering of 4′-cyanophenyl-4-alkylbenzoates by ^{13}C NMR", *Liq. Cryst.* **14**, 591-601, 1993.

18. B. Deloche, B. Cabane and D. Jerome, "Effect of Pressure on the Mesomorphic Transitions in Para-Azoxyanisole (PAA)", *Mol. Cryst. Liq. Cryst.*, **15,** 197-209, 1971.

19. G.P. Wallis and S.K. Roy, "Nuclear magnetic resonance studies of liquid crystals under pressure", *J. Phys.*, **41**, 1165-1172, 1980.